Characteristics of Phase-Shifted Fiber Bragg Grating Inscribed by Fusion Splicing Technique and Femtosecond Laser

Yajun Jiang[1,2], Jian Xu[1,2], Yuan Yuan[1,2], Dexing Yang[1,2], Dong Li[1,2], Meirong Wang[1,2] and Jianlin Zhao[1,2]

[1]*Key Laboratory of Space Applied Physics and Chemistry, Ministry of Education, Xi' an, China*

[2]*Shaanxi Key Laboratory of Optical Information Technology, School of Science, Northwestern Polytechnical University Xi' an 710072, China*

Keywords: Optical Fiber Sensors, Phase-shifted Fiber Bragg Gratings, Femtosecond Laser.

Abstract: Phase-shifted fiber Bragg grating (PS-FBG) inscription in nonphotosensitive single mode fiber (SMF) by the fusion splicing technique and femtosecond laser is reported. Two SMFs are fusion spliced to introduce a refractive index modulation point which acts as a phase shift, then exposing the fusion spliced fiber with femtosecond laser and a uniform phase mask. Two dips can be observed in the transmission spectrum of inscribed grating, and the max induced refractive index modulation can reach to 4.2×10^{-4} without any fiber sensitization for a peak power density of 4.5×10^{13} W/cm^2. The annealing tests show that type I PS-FBG is successfully inscribed. This type of grating also shows good strain and pressure characteristics. Such PS-FBGs can be potentially used for optical fiber lasers, filters and sensors.

1 INTRODUCTION

Phase-shifted fiber Bragg gratings (PS-FBGs) show a very narrow transmission band within its reflection spectrum, and they have found many applications in wavelength-division multiplexing systems (Agrawal and Radic, 1994), optical fiber lasers (Chen et al., 2005), high finesse transmission filters (Zou et al., 2013), ultrasonic detectors (Rosenthal et al., 2011; Liu and Ham, 2012) and optical fiber sensors (Malara et al., 2015). Many methods have been presented for PS-FBG inscription, such as employing a phase-shifted phase mask (PM) (Liu and Ham, 2012), Moiré method by slightly tuning the laser wavelength (Malara et al., 2015) or shifting the fiber perpendicularly to the fiber axis (Reid et al., 1990), moving fiber-scanning beam technique (Cole et al., 1995), post-processing technique by exposing the uniform FBG with focused UV (Canning and Sceats, 1994) or CO_2 laser (Xia et al., 2005), and exposing twice process (Chehura et al., 2010), in which two uniform FBGs with same parameters are overlapped physically by one grating period. These methods mentioned above possess good repeatability, flexibility and quality, but they need the relatively expensive phase-shifted PM or a high precise control or the PS-FBGs show poor annealing properties.

In the past decades, femtosecond laser has been explored for writing complex FBGs in many types of fibers (Thomas et al., 2008; Marshall et al., 2010; Williams et al., 2011). PS-FBG has been inscribed by point-by-point technique with femtosecond laser by modulating the phase and frequency of femtosecond laser with two triggers (Marshall et al., 2010) or an electro-optical modulator (Burgmeier et al., 2014) in conjunction with a high precise stage, this technique is versatile and repeatable; however, it requires the synchronization of pulse train with the writing position. The PS-FBG has be also inscribed by introducing an in-grating bubble in the middle of uniform FBG with femtosecond laser and fusion splicing technique (Liao et al., 2013), in which the phase shift is adjusted by filling liquids with different refractive indices into the bubble, whereas the fabrication process is complex. Another PS-FBG inscription technique is proposed by overexposing a uniform FBG with femtosecond laser and a uniform PM (He et al., 2015), which is easy to implement, but an obvious decrease in the transmission loss at the Bragg wavelength is observed during the inscription process.

In this paper, a new method for PS-FBG inscription in nonphotosensitive single mode fiber

Jiang, Y., Xu, J., Yuan, Y., Yang, D., Li, D., Wang, M. and Zhao, J.
Characteristics of Phase-Shifted Fiber Bragg Grating Inscribed by Fusion Splicing Technique and Femtosecond Laser.
DOI: 10.5220/0005738503560360
In *Proceedings of the 4th International Conference on Photonics, Optics and Laser Technology (PHOTOPTICS 2016)*, pages 358-362
ISBN: 978-989-758-174-8
Copyright © 2016 by SCITEPRESS – Science and Technology Publications, Lda. All rights reserved

(SMF) by fusion splicing technique and femtosecond laser is reported. The PS-FBG is inscribed by fusion splicing two SMFs and then exposing the fusion spliced fiber with femtosecond laser and a uniform PM. Its annealing, strain and pressure characteristics are experimentally studied.

2 EXPERIMENTAL SETUP

The inscription process is divided into three steps. First, the SMF (Coring SMF-28e+) is cleaved into two sections by using an optical fiber cleaver after stripping its coating with a length of about 20 mm. Then the two sections are spliced by a fusion splicer, and the typical fusion loss is 0.01 dB. Finally, the fusion spliced fiber is exposed by femtosecond laser through a cylindrical lens and a uniform PM. Figure 1 shows the schematic diagram of the PS-FBG inscription by femtosecond laser. The femtosecond laser pulses have a 35 fs duration and are generated by a Ti:sapphire amplifier at wavelength of 800 nm with pulse repetition rate of 1 kHz. The max output pulse energy of 4 mJ can be adjusted by rotating a half-wave plate followed by a polarizer. The laser beam has a radius of 4 mm and is focused by the cylindrical lens with focal length of 40 mm through a zero-order nulled PM onto the fiber. The half-width of the focal line ω is 2.5 μm according to $\omega=\lambda f/(\pi\omega_0)$, where λ is the wavelength, f is the focal length of the cylindrical lens, and ω_0 is the incident beam radius. The coating stripped SMF is cleaved and spliced, and then it is positioned behind the PM at a distance of about 2 mm in order to produce two-pure interference (Smelser et al., 2004). The PM is designed for 800 nm radiation with a period of 2142 nm (Ibsen Photonics) which is twice of the period of inscribed PS-FBG. Less than 5% of the beam is diffracted into the 0th order, and more than 70% of the beam is diffracted into the ±1st orders. The

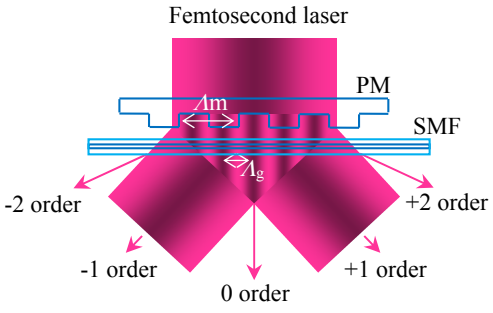

Figure 1: Schematic diagram of the PS-FBG inscription by femtosecond laser.

during the inscription process by an ASE source and an optical spectrum analyzer.

3 RESULTS AND DISCUSSIONS

The fusion spliced fiber is exposed by 600 μJ laser pulses for 100 s and the peak power density at the focus is about 4.1×10^{13} W/cm^2. Figure 2 gives the reflection and transmission spectra of the induced PS-FBG. We can see that there are two main dips in the transmission spectrum because the PS-FBG is successfully inscribed. A refractive index modulation point is introduced by fusion splicing two SMFs in the fiber core, which acts as a phase shift during the inscription process. The 2nd order PS-FBG is inscribed according to the Bragg condition defined by $m\lambda_{Bragg}=2n_{eff}\Lambda_g$, where λ_{Bragg} is the Bragg wavelength, m is the order number, n_{eff} represents the effective index of fiber core, and Λ_g donates the grating period. The measured Bragg wavelength λ_{Bragg}=1548.1 nm, so the calculated n_{eff}=1.445. The phase shift is observed during the whole inscription process which is different from the PS-FBG formation in stage II (He et al., 2015), and it is almost unchanged. The cladding modes are also observed due to the light coupling into the fiber cladding, which can be suppressed by scanning the inscription laser beam vertically to maximize coverage of the fiber core region.

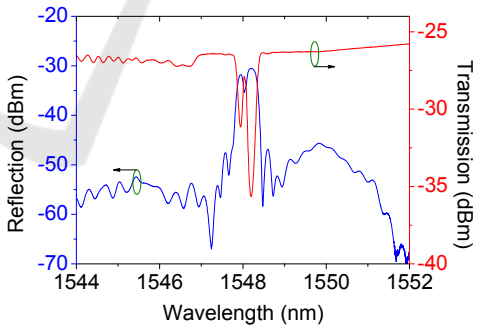

Figure 2: Reflection and transmission spectra of the PS-FBG inscribed by femtosecond laser.

During the inscription process, the wavelengths show a nonlinear red shift for about 0.14 nm with the exposure time (total incident laser fluence). The transmission losses of the 1st and 2nd dips increase to -9.3 dB and -4.8 dB, while the wavelengths shift to 1548.20 nm and 1547.94 nm, respectively. No obvious saturation is observed within 100 s. The induced refractive index modulation can be inferred from the expression for maximum reflectivity

$R=\tanh^2(\kappa L)$, where the coupling coefficient $\kappa=\pi m\Delta n_m/(2n_{eff}\Lambda_m)$, L is the grating length, Δn_m is the refractive index modulation of the mth order grating, and Λ_m is the PM period. So the induced refractive index modulation $\Delta n_m=3.3\times10^{-4}$ for a dip of -9.3 dB. The fiber core's refractive index n_{eff} at the fusion spliced point decreases within few hundreds of micronmeters due to dopant diffusion, glass structure change and residual stress relaxation (Abrishamian et al., 2012), so negative refractive index change in the fusion spliced point is introduced to form a PS-FBG during the inscription process. The insertion loss at 1550 nm is about 0.3 dB.

The annealing tests are conducted in a tube furnace. The evolution of the transmission spectra of PS-FBG form 24 ˚C to 940 ˚C are shown in Fig. 3. It can be seen that the transmission spectrum of PS-FBG shifts to long wavelength, at the same time, it transmission decreases with increase the temperature. The change of the central wavelengths and the transmission losses with the temperature are given in Fig 4 (a) and (b), respectively. It can be seen that the central wavelengths of the two dips shift almost with the same speed according to the polynomial fit results. But the transmission loss of the 2nd dip changes slowly compared with the 1st dip. There is a turning point near the temperature of 800 ˚C at which the loss of the 2nd dip is larger than the 1st one. At the same time a new third dip can be observed, its loss increases firstly and approaches to the 2nd one at the temperature of 920 ˚C, and then they decrease at the same speed. The experimental results show that type I PS-FBG has been inscribed.

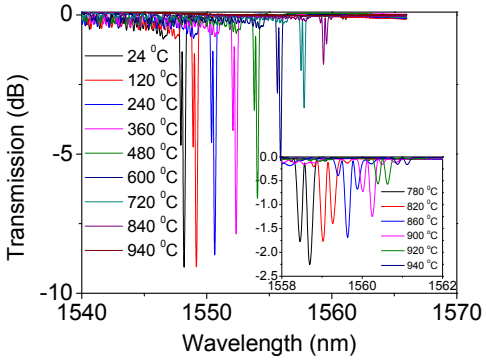

Figure 3: Evolution of the transmission spectra of PS-FBG under different temperature.

The hydrostatic pressure test of the PS-FBG was performed in a sealed stainless steel tube filled with water. The transmission loss of the PS-FBG is about -13 dB, so the induced refractive index modulation $\Delta n_m=4.2\times10^{-4}$. Figure 5 gives the evolution of the transmission spectra of PS-FBG under different pressures in the range from 0 MPa to 25 MPa with a step of 5 MPa. It can be seen that the transmission

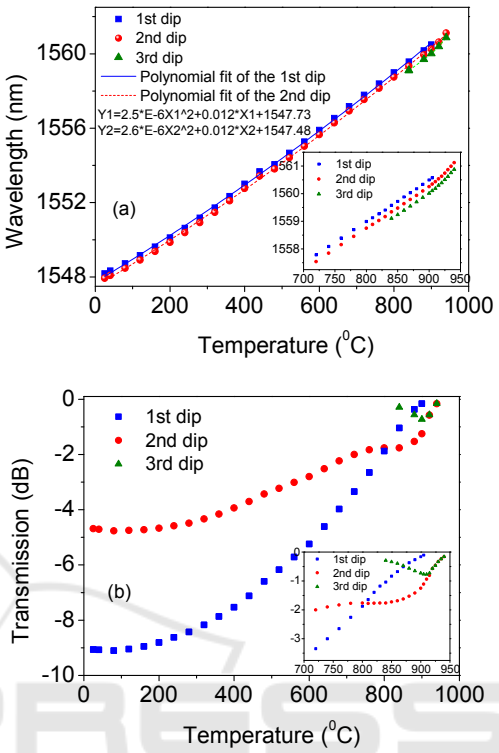

Figure 4: Change of the (a) central wavelengths and (b) transmission losses for two dips with the temperature.

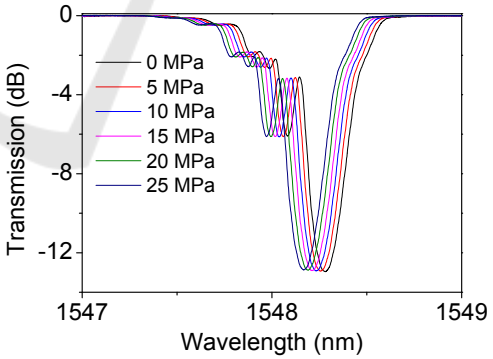

Figure 5: Evolution of the transmission spectra of PS-FBG under different pressures.

spectrum has a blue shift and its shape is not distorted during increasing the pressure. Figure 6 depicts the central wavelengths and transmission losses for the two dips under different pressures. From Fig. 6 (a), we can see that the central wavelengths for two dips decrease linearly with the pressure at a same sensitivity of -4.4 pm/MPa, which is slightly higher than that of the UV laser induced

FBG in standard SMF. There is no hysteresis for both increasing and decreasing cycles. In Fig. 6 (b), the transmission losses of the two dips are almost unchanged under different pressures, and the fluctuation is only about ± 0.1 dB.

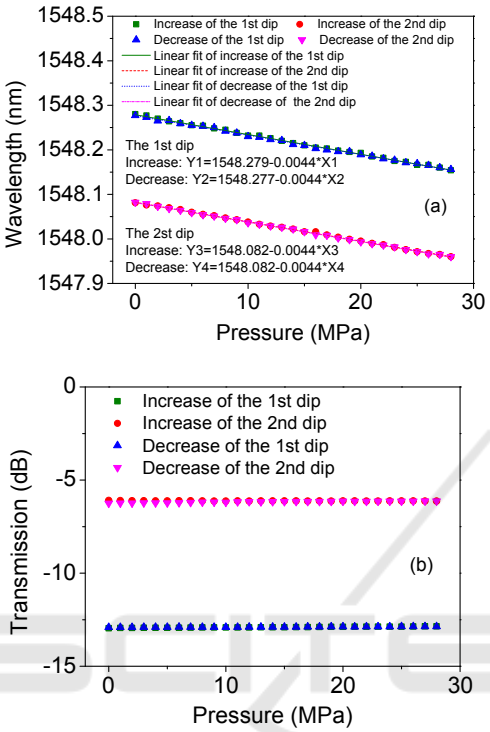

Figure 6: Changes of the (a) central wavelengths and (b) transmission losses for two dips under different pressures.

The strain test of another PS-FBG with the dip of -11.6 dB inscribed under the same condition was performed by fixing it on two manual translating stages with a resolution of 0.01 mm, and the space between the two fixed points was 483 mm. The strain was applied on the FBG by adjusting one of the translating stages up to 1 mm with a step of 0.05 mm. Figure 7 shows the evolution of the transmission spectra under different strains in the range from 0 με to 2070 με. We can see that the transmission spectrum has a red shift and there is no distortion during increasing the strain. Figure 8 (a) and (b) depict the wavelengths shift for two dips under different strains. We can see that the strain response of the PS-FBG shows good linearity and repeatability, and the strain sensitivity is 1.2 pm/με, which is the same with that of the UV laser induced FBG. But the transmission loss of the 1st dip decreases when increasing the strain, while it increases for the 2nd one.

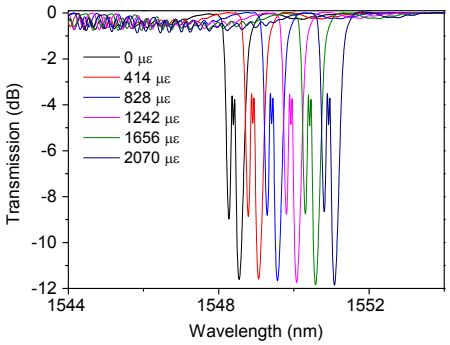

Figure 7: Evolution of the transmission spectra under different strains.

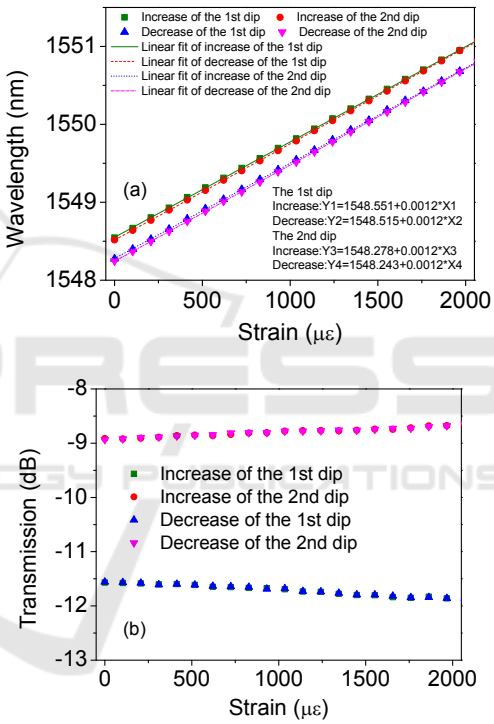

Figure 8: Change of the (a) central wavelengths and (b) transmission losses for two dips under different strains.

4 CONCLUSIONS

In conclusion, PS-FBGs have been successfully inscribed in nonphotosensitive SMFs by fusion splicing technique and femtosecond laser through a uniform PM. Two main dips can be observed due to the formation of PS-FBG and its transmission spectrum of PS-FBG shows a nonlinear red shift during the inscription process. The max induced refractive index modulation of 4.2×10^{-4} is achieved for a PS-FBG with a dip of -13 dB for a peak power

density of 4.5×10^{13} W/cm^2. The annealing, strain and pressure characteristics of the PS-FBG are experimentally studied. These PS-FBGs inscribed in SMFs by femtosecond laser will find applications in optical fiber lasers, two wavelength filters and optical fiber sensors.

ACKNOWLEDGEMENTS

This work was supported by the National Natural Science Foundation of China (Grant No. 61405163), the Fundamental Research Funds for the Central Universities (Grants No. 3102014KYJD025, 3102014JCQ01100 and 3102015BJ(Ⅱ)ZS015) and the Northwestern Polytechnical University Foundation for Fundamental Research (Grant No. JC20110272).

REFERENCES

Agrawal, G & Radic, S 1994, 'Phase-shifted fiber Bragg gratings and their application for wavelength demultiplexing', *IEEE Photonics Technology Letters*, vol. 6, no. 8, pp. 995-997.

Chen, X, Yao, J & Deng, Z 2005, 'Ultranarrow dual-transmission-band fiber Bragg grating filter and its application in a dual-wavelength single-longitudinal-mode fiber ring laser', *Optics Letters*, vol. 30, no. 16, pp. 2068-2070.

Zou, X, Li, M, Pan, W, Yan, L, Azaña, J & Yao, J 2013, 'All-fiber optical filter with an ultranarrow and rectangular spectral response', *Optics Letters*, vol. 38, no. 16, pp. 3096-3098.

Rosenthal, A, Razansky, D & Ntziachristos, V 2011, 'High-sensitivity compact ultrasonic detector based on a π-phase-shifted fiber Bragg grating', *Optics Letters*, vol. 36, no. 10, pp. 1833-1835.

Liu, T & Han, M 2012, 'Analysis of π-phase-shifted fiber Bragg gratings for ultrasonic detection', *IEEE Sensors Journal*, vol. 12, no. 7, pp. 2368-2373.

Malara, P, Campanella, C, De Leonardis, F, Giorgini, A, Avino, S, Passaro, V & Gagliardi, G 2015, 'Enhanced spectral response of pi-phase shifted fiber Bragg gratings in closed-loop configuration', *Optics Letters*, vol. 40, no. 9, pp. 2124-2126.

Reid, D, Ragdale, C, Bennion, I, Buus, J & Stewart, W 1990, 'Phase-shifted Moiré grating fibre resonators', *Electronics Letters*, vol. 26, no. 1, pp. 10-12.

Cole, M, Loh, W, Laming, R, Zervas, M & Barcelos, S 1995, 'Moving fibre/phase mask-scanning beam technique for enhanced flexibility in producing fibre gratings with uniform phase mask', *Electronics Letters*, vol. 31, no. 17, pp. 1488-1490.

Canning, J & Sceats, M 1994, 'π-phase-shifted periodic distributed structures in optical fibres by UV post-processing', *Electronics Letters*, vol. 30, no. 16, pp. 1344-1345.

Xia, L, Shum, P & Lu, C 2005, 'Phase-shifted bandpass filter fabrication through CO_2 laser irradiation', *Optics Express*, vol. 13, no. 15, pp. 5878-5882.

Chehura, E, James, S & Tatam, R 2010, 'A simple and wavelength-flexible procedure for fabricating phase-shifted fibre Bragg gratings', *Measurement Science & Technology*, vol. 21, no. 9, pp. 094001-1-7.

Thomas, J, Voigtländer, C, Schimpf, D, Stutzki, F, Wikszak, E, Limpert, J, Nolte, S & Tünnermann, A 2008, 'Continuously chirped fiber Bragg gratings by femtosecond laser structuring', *Optics Letters*, vol. 33, no. 14, pp. 1560-1562.

Marshall, G, Williams, R, Jovanovic, N, Steel, M & Withford, M 2010, 'Point-by-point written fiber-Bragg gratings and their application in complex grating designs', *Optics Express*, vol. 18, no. 19, pp. 19844-19859.

Williams, R, Voigtländer, C, Marshall, G, Tünnermann, A, Nolte, S, Steel, M & Withford, M 2011, 'Point-by-point inscription of apodized fiber Bragg gratings', *Optics Letters*, vol. 33, no. 15, pp. 2988-2990.

Burgmeier, J, Waltermann, C, Flachenecker, G & Schade, W 2014, 'Point-by-point inscription of phase-shifted fiber Bragg gratings with electro-optic amplitude modulated femtosecond laser pulses', *Optics Letters*, vol. 39, no. 3, pp. 540-543.

Liao, C, Xu, L, Wang, C, Wang, D, Wang, Y, Wang, Q, Yang, K, Li, Z, Zhong, X, Zhou, J & Liu, Y 2013, 'Tunable phase-shifted fiber Bragg grating based on femtosecond laser fabricated in-grating bubble', *Optics Letters*, vol. 38, no. 21, pp. 4473-4476.

He, J, Wang, Y, Liao, C, Wang, Q, Yang, K, Sun, B, Yin, G, Liu, S, Zhou, J & Zhao, J 2015, 'Highly birefringent phase-shifted fiber Bragg gratings inscribed with femtosecond laser', *Optics Letters*, vol. 40, no. 9, pp. 2008-2011.

Smelser, C, Grobnic, D & Mihailov, S 2004, 'Generation of pure two-beam interference grating structuresin an optical fiber with a femtosecond infrared source and a phase mask', *Optics Letters*, vol. 29, no. 15, pp. 1730-1732.

Abrishamian, F, Dragomir, N & Morishita, K 2012, 'Refractive index profile changes caused by arc discharge in long-period fiber gratings fabricated by a point-by-point method', *Applied Optics*, vol. 51, no. 34, pp. 8271-8276.